GATE Air–Sea Interaction. I: Numerical Model Calculation of Local Sea-Surface Temperatures on Diurnal Time Scales Using the GATE Version III Gridded Global Data Set

P. S. BROWN, JR., J. P. PANDOLFO AND S. J. THOREN

The Center for the Environment and Man, Inc., Hartford, CT 06120

(Manuscript received 3 August 1981, in final form 25 January 1982)

ABSTRACT

The numerical model of air–sea interaction previously described in Jacobs (1978), Pandolfo and Jacobs (1972) and Pandolfo (1969) is inserted at one horizontal grid point in the GATE III Gridded Global Data Set to calculate a model-generated, local interface temperature over a two-day interval (0000 GMT 4 September–0000 GMT 6 September 1974) of GATE Period III.

The experiment provides a preliminary demonstration of the accuracy achievable in predicting sea-surface temperature over multi-day scales with limited-domain models nested within global data sets. It also demonstrates the degree of sensitivity of the model-generated sea-surface temperature to the inclusion of parameterized convective adjustments in the oceanic and atmospheric sub-layers under the general conditions prevailing during the period studied.

Initial and boundary data were provided to the local model on a relatively coarse vertical grid and with relatively coarse (12 h) temporal resolution. Linear spatial and temporal interpolation was used to produce the higher resolution data required by the model. (A 6 min time step and grid intervals as small as 1 m were used in the experiments described in this paper.) Therefore, the nested local model provides, in this preliminary experiment, increased resolution only in the vertical and temporal dimensions. It also adds greater physical complexity to the global-scale model used in the generation of the GATE III gridded data set (and described in Miyakoda *et al.*, 1980) by coupling the atmosphere–ocean boundary layers to allow the prediction (rather than the prespecification) of sea-surface temperature, and by taking into account model-generated temporal variations in the vertical structures of the atmospheric transmissivity with regard to solar and infrared radiation.

The two-day period used for this demonstration is characterized by moderately disturbed tropical marine conditions with intermittent periods of light wind as contrasted to the generally steady trade-wind and midlatitude conditions previously treated in the papers cited above. Nevertheless, the air–sea interaction model, when suitably refined to include parameterized convective adjustment in the coupled air–ocean layers, again yields model-generated sea-surface temperatures which generally differ from those observed by less than the uncertainty of measurement, and with accuracy well within that estimated in Charney *et al.* (1966) as required in order to extend the temporal range of weather forecasts in numerical models of the atmosphere.

In one model run of the experiment the atmospheric convective adjustment was eliminated from the model. The result is an unrealistic accumulation of heat in the ocean surface layer. In another model run of the experiment the ocean-surface layer convective adjustment was eliminated from the model. The result is a somewhat cooler model-generated nighttime interface temperature.

Interaction between the parameterized convective processes of the coupled air–sea model layers is also evident from the results. When the parameterized atmospheric convective adjustment is omitted from the model, significant alteration of the model-generated oceanic "convection depth" takes place; conversely when the parameterized oceanic convective adjustment is omitted, there occurs a substantial alteration of the model-generated atmospheric "convective condensation level."

1. Introduction

Among the stated findings of the GARP Atlantic Tropical Experiment are that: energetically important (in an atmospheric context) variations of sea-surface temperature (SST) have been observed on the 3–6 day time scale (Krishnamurti *et al.*, 1979); diurnal ranges of GATE open-ocean SST occasionally approach 1°C (Peters, 1978); important diurnal variations in the hydrologic cycle of the tropical marine atmosphere have been detected (McGarry and Reed, 1978; Gray and Jacobson, 1977); and that differential diurnal heating of land and ocean is an important factor in the accurate simulation of storm development in a tropical numerical weather prediction model (Krishnamurti *et al.*, 1979).

This last result indicates that linkages between land, atmosphere and ocean on these time scales may be reproducible in numerical models, even though they are difficult to discern in standard oceanographic measurement and analysis.

On the other hand, there have been stated findings (Greenfield and Fein, 1979) of the GATE oceanic sub-program that "the time scale of variability of the

0022-3670/82/050483-12$07.00

SST is generally of the order of weeks;" and that "meteorological events with time scales of a day or two . . . evoke no discernible response within the surface layers of the eastern Tropical Atlantic Ocean." While these findings may be valid in an oceanic context, they do not preclude the possibility that significant weather changes are energetically consistent with much smaller heat-content changes in much shallower oceanic surface layers than are normally of concern to oceanographers.

There have been previous demonstrations of the capability of the numerical air–sea interaction model used in this study. Pandolfo (1969, 1971), Pandolfo and Jacobs (1972), and Jacobs (1978) report its application in cases characterized by steady, moderate wind speeds, and time-constant cloudiness. Data collected during the GARP Atlantic Tropical Experiment (GATE) have recently become available, which include periods with intermittently light wind speeds and large variations of cloud and rain. It is one such period which is the object of study in the work described here, *viz.*, a 48-h period during Phase III of GATE from 0000 GMT, 4 September to 0000 GMT, 6 September 1974.

Tests of the model in these conditions led to some refinement of the calculation algorithms used for the model (described in Section 2). Analysis of the algorithms led to the derivation of some general characteristics of finite-difference forms of the advective–diffusive partial differential equations which form the core of "primitive equation" models, [Brown and Pandolfo, 1978, 1979, 1980, 1982]. The tests have also allowed the exploration of a local interactive link between thermal convection in the atmosphere and ocean (see Section 3c). From the experiments there has emerged a preliminary picture of the problems to be overcome and the potential accuracy to be attained in extending this type of model to three dimensions and in lengthening the temporal integration period (see Section 4 below).

To this extent the work described here was intended to contribute directly to the achievement of the second basic objective of the GATE Central Programme, *viz.*, "to facilitate the development of numerical modeling and prediction methods" (Houghton, 1974).

2. The air–sea interaction model

a. The basic structure

The fully coupled air–sea interaction model of Pandolfo (1969) forms the core of the experimental model used here. The basic equations take the form

$$\frac{\partial}{\partial t} x_i + \mathbf{V} \cdot \mathbf{G}_i = \frac{\partial}{\partial Z}\left[K_i(\mathrm{Ri}, Z)\frac{\partial x_i}{\partial Z}\right] + F_i \qquad (i = 1, 2, \cdots 8). \qquad (1)$$

The dependent variables x_i and the associated quantities are

i	x_i	F_i
1	u_A	$f[v_A - v_g(Z)]$
2	v_A	$f[u_g(Z) - u_A]$
3	T_A	$\Gamma\partial K_3/\partial Z + S_R$
4	q	0
5	u_w	$f[v_w - v_g(Z)]$
6	v_w	$f[u_g(Z) - u_w]$
7	T_w	0
8	s	0

The symbols are defined as follows:

u_A eastward component of wind
v_A northward component of wind
T_A air temperature
q specific humidity
u_w eastward component of current
v_w northward component of current
T_w water temperature
s salinity
$\mathbf{V}$ horizontal velocity vector
$\mathbf{G}_i$ horizontal gradient vector for the unknown variable
K_i appropriate eddy-exchange coefficient for the unknown variable
f Coriolis parameter
u_g eastward component of the geostrophic velocity
v_g northward component of the geostrophic velocity
Γ atmospheric adiabatic lapse rate (= 0.98 $\times 10^{-4}$ K cm^{-1})
Ri Richardson number
Z the height coordinate, with origin at the air/sea interface
S_R temperature source term due to convergence of the infrared radiative flux.

As implied by (1), closure is achieved by the adoption of "K theory" with exchange coefficients that are stability- and wave-dependent. Details of the K formulations are set forth by Pandolfo (1969) and Jacobs (1978, Form I).

The second reference cited contains an extended discussion of the simultaneous treatment of two-scaling lengths, *viz.*, the Monin-Obukov "stability" length, and the Kitaigorodsky "turbulent wave" length in the formulation of the atmospheric and oceanic numerical mixing models. The results presented there show that direct and indirect interactions between only these two model elements are sufficiently complex to produce solution features that

are not amenable to physically intuitive consideration or analysis in terms of simple closed-form mathematics.

The model includes as one component stepwise recalculation of cloud- and moisture-dependent solar, telluric and atmospheric radiation as the solution proceeds. The radiative parameterization used was first outlined in Atwater (1972) and Atwater and Brown (1974) and has been recently refined and modified as described in, e.g., Ball *et al.* (1981).

The calculation of depth-dependent absorption of solar radiation in the ocean layers uses the absorption parameters derived by Paulson and Simpson (1977) for a two-band approximation to the solar irradiance spectrum.

The model includes, as another component, parameterized calculation of vertical turbulent mixing in the atmospheric boundary layer as described in Pandolfo (1969, 1971); and in the ocean boundary layer as described in Pandolfo (1969) and Jacobs (1978). This turbulent transfer is conventionally supplemented in atmospheric numerical prediction models by parameterization of the effects of convective cloud and precipitation formation on vertical transfer [see, e.g., Lyne *et al.* (1976), Krishnamurti *et al.* (1979), Kreitzberg and Perkey (1976), Miyakoda and Sirutis (1977), and Arakawa and Schubert (1974)]. The local air–sea interaction model used here includes (in its atmospheric portion) parameterized convective adjustment which is summarily described in Section 2b.

Much work has been done on one-dimensional modeling of the oceanic mixed layer in which the integral properties of the layer are predicted from a more or less physically complete formulation of its heat budget and turbulent structure [see, e.g., Kraus and Turner (1967), and for a review Niiler and Kraus (1977)]. Less conventional is the use of parameterization of convection in a spatially gridded model of the ocean surface layer in the presence of penetrative solar radiation. A convective adjustment procedure, analogous to that used in the atmosphere, and based on the work of Dalu and Purini (1981), to account for this process is also described in Section 2b.

A numerical prediction model for the coupled air–sea boundary layers must include interface coupling conditions that are extensions of those conventionally applied in numerical models of the atmosphere or of the ocean. We repeat here the specification of the interface conditions listed first in Pandolfo (1969). These require continuity of eastward and northward velocity and of temperature, and saturation of the air layer at the modeled interface. They also require continuity of the turbulent frictional stress components and equivalence of the net evaporation–precipitation on the air side with turbulent vertical salinity flux on the water side of this interface. These conditions close the problem of solving a quartic equation in the air–water interface temperature that results from requiring balance of the vertical heat fluxes on both sides of the modeled interface at each time step of the numerical integration, through an iterative procedure (Jacobs and Brown, 1973).

b. The convective adjustments

Early mesoscale models of the convection process were developed by Kasahara (1961), Lilly (1962) and others. Experiments with these models showed that the solutions deteriorated rapidly since the grid-scale convection could not be resolved by the grid itself. Manabe *et al.* (1965) later introduced a convective parameterization procedure to achieve more realistic results. These parameterizations, which account for the bulk effects of moist convection on the production of cloud and precipitation, are used to treat the atmospheric layer of our air/sea interaction model.

In the case in which the model-scale predicted values of temperature and humidity indicate supersaturation and a grid-layer lapse rate that is more stable than the moist-adiabatic, no parameterization is required. A straightforward adjustment of the predicted values to yield saturation, with concurrent condensation, latent heating and rain-out of the excess water, according to the scheme of McDonald (1963) is carried out. Generalization of the scheme allows convective adjustment in the presence of subsaturated model-scale conditions, if the presence of a "Convective Condensation Level" (CCL) is diagnosed in the unadjusted model solutions. It also allows diagnosis of the corresponding fractional area coverage by the parameterized convection which determines the degree of latent heating, atmospheric drying and radiative modulation effected by the parameterized "cloud and rain-out." Reports on global-scale climate models which include some aspects of this generalization have recently become available (e.g., Ramanathan and Dickinson, 1981; Shukla and Sud, 1981; and Wetherald and Manabe, 1981).

It should be noted that the detailed form of our generalizations differs from those reported above because of the greater vertical resolution and physical generality of the air-sea interaction model when compared to global-scale general circulation models of the type described, e.g., in Manabe *et al.* (1965). The adjustment is generally applied, as in Manabe *et al.*, by first making a prediction of model-scale dependent variables at each time step, and then determining whether certain prespecified criteria on their values and vertical distributions are met. If they are, a final adjustment of the predicted model scale temperature and humidity values is carried out. The prediction is then carried forward from these adjusted values.

The specific generalizations require first a basic

assumption that the model-scale value of a variable represents the mean of a range of values produced by sub-model scale (in space or time) phenomena. They then require quantitative estimates of some characteristic upper and lower values that range about the model-scale mean. These estimates should be consistent with the model's physical and numerical properties.

Once these estimates are obtained, a particular grid level is identified as a CCL if its upper characteristic value of humidity is equal to or exceeds the saturation value of a parcel lifted adiabatically through a characteristic length and starting from the model-scale value of temperature at the parcel "level of origin." For purposes of identification of a CCL only, the characteristic length is the turbulent mixing length defined by

$$l_i = (K_i/S_i)^{1/2} \leqslant Z_i\,, \tag{2}$$

where S is the magnitude of the vertical wind shear vector. Subscripts serve to index the grid level at which the variables are evaluated. The upper and lower characteristic values of humidity are the maximum and minimum model-scale values encountered within the layer defined by the heights

$$Z_i \pm l_i\,. \tag{3}$$

Once a given grid level is identified as a CCL, it defines a parameterized "cloud base" level,

$$Z_B \equiv Z_i\,. \tag{4}$$

Each grid level Z_i in turn, above this level is tested until the temperature T_i satisfies the inequality

$$T_i \geqslant T_B + \Gamma_M(Z_i - Z_B), \tag{5}$$

where Γ_M is the moist adiabatic lapse rate; i.e., the test is performed until a parameterized "cloud top" level is found.

At the intermediate parameterized "cloud" levels, the heat required to adjust the "in-cloud" lapse rate between adjacent grid levels from the model-scale lapse rate

$$\Gamma = (T_{i-1} - T_i)(Z_i - Z_{i-1})^{-1}, \tag{6}$$

to the moist adiabatic lapse rate Γ_M is given by

$$\Delta H_i = \tfrac{1}{2}C\rho_i[T_{i-1} + \Gamma_M(Z_i - Z_{i-1}) - T_i](Z_{i+1} - Z_{i-1}), \tag{7}$$

and the temperature adjustment corresponding to this heat source for the grid layer containing Z_i is

$$\Delta T_i = \frac{2\Delta H_i}{C\rho_i(Z_{i+1} - Z_{i-1})}\,. \tag{8}$$

Here C is the specific heat of air at constant pressure and ρ_i is the air density at grid level i. If L is defined as the latent heat of evaporation, the corresponding condensed specific water is

$$\Delta q_i = C\Delta T_i/L. \tag{9}$$

To estimate the fraction F of the model-scale horizontal dimension occupied by parameterized "cloud," we use again the concept of upper, lower and mean (model-scale) model characteristic values of specific moisture content to obtain

$$F_i = (q_i - q_{i-})/(q_{i+} - q_{i-}) \leqslant 1, \tag{10}$$

where q_+ is now defined as the specific moisture content of a parcel undergoing moist-adiabatic ascent from Z_B to the level Z_i, i.e.,

$$q_{i+} = q_{s,i} + \Delta q_i\,, \tag{11}$$

where $q_{s,i}$ is the saturation value at pressure P_i and temperature $T_{i-1} + \Gamma_M\,(Z_i - Z_{i-1})$, and q_{i-} is the lower value characteristic of the cloud-free environment and estimated as outlined previously for the sub-cloud layer. However, if the model scale humidity is supersaturated, F_i is set to unity.

The final adjustment, therefore, requires increasing the model scale temperature at the grid level Z_i by $F_i\Delta T_i$, decreasing the specific humidity in the modeled atmospheric layer by an integral amount commensurate with $F_i\Delta q_i$ and some "entrainment" hypothesis and by "raining out" water at a rate

$$\mathrm{Ri} = \rho_i\Delta q_i(Z_{i+1} - Z_{i-1})(2\Delta t)^{-1} \text{ per unit area}, \tag{12}$$

where Δt is the time increment used in the numerical integration procedure.

The entrainment hypothesis that appears to be most effective (when used in conjunction with the spatial and temporal resolution and other parameterizations of this model) removes vapor only from grid layers below the ith (cloud) level, and distributes the vapor sink among these layers in proportion to the ratio of the individual grid-layer specific humidity to the mass-weighted vertically averaged specific humidity of these layers. Thus, the adjusted specific humidity q'_j is given by

$$q'_j = q_j\{1 - \mathrm{Ri}2\Delta t[\tilde{q}\rho_j(Z_{j+1} - Z_{j-1})]\}^{-1}, \quad A \leqslant j \leqslant i-1, \tag{13}$$

where

$$\tilde{q} = [\sum_{j=A}^{i-1} \rho_j q_j(Z_{j+1} - Z_{j-1})] \times [\sum_{j=A}^{i-1} \rho_j(\Delta Z_{j+1} - \Delta Z_{j-1})]^{-1}. \tag{14}$$

The calculations are repeated for each intermediate cloud level at a given time step; the final "rain

out" rate for the time step is obtained by the sum

$$R_T = \sum_{i=A}^{H} \mathrm{Ri}, \tag{15}$$

and the adjustment of q_j for each sub-cloud grid layer is repeated for each additional cloud level diagnosed.

The oceanic convective adjustment is applied in a similar manner, by first making a prediction of the model-scale dependent variables at each time step, including a diagnostic calculation of the interface temperature by iterative solution of the interface heat balance equation, (Jacobs and Brown, 1973), and accounting for, at sub-surface levels, the effects of horizontal and vertical model-scale advection, shear and wind-wave generated smaller scale turbulence, and radiative absorption. Then if certain prespecified criteria on the computed values of the heat sources and sinks of the upper ocean layers are satisfied, the presence and thickness of a "convection depth" D, as identified in Dalu and Purini (1981) (DP), are diagnosed. Necessary conditions for the existence of D are those specified in DP and generally require past or present positive buoyant energy production in the upper ocean layers from the interface heat fluxes and the penetrative solar radiation flux. The existence of D also requires that there has been no thermocline shallower than D but that there be a density profile which is statically stable (through depth D) as a result of surface mixing to the depth D.

Given these conditions, the depth D is defined as the depth at which the vertical convergence of the radiative flux $S(Z)$, defined in closed form as in Paulson and Simpson (1977), balances the sum of the surface fluxes removing heat at the interface, i.e., as the depth which satisfies the condition [DP, Eq. (6)],

$$\frac{S(Z) - G}{D} = \frac{\partial S(Z)}{\partial Z}, \tag{16}$$

where G is the net sum of the interface fluxes, i.e.,

$$G = I_A - LE - C_A - \sigma T_0^4, \tag{17}$$

with I_A the atmospheric (downward) radiative flux at the interface, E the evaporative flux at the interface, C_A the sensible heat flux between atmosphere and interface, and σ the Stefan-Boltzmann constant.

In our adaptation of the parameterization we do not proceed with the convective adjustment unless these conditions have been met. In their absence, the model proceeds as a spatially gridded model in Eulerian "primitive equation" form. At each time step that the conditions are met, the predicted oceanic temperature is adjusted to result in uniformly mixed heat content from the interface to the effective depth D, and the model predictions proceed from this adjusted temperature.

c. *Mathematical aspects of the numerical integration procedure*

The basic prognostic partial differential equations of the model are integrated with the use of an implicit space-centered three-time-level scheme to approximate fluxes in the vertical direction. The basic scheme for treatment of the diffusion equation is suggested and briefly described in Richtmyer and Morton (1967; Scheme No. 9, p. 190). Some of the problems arising from generalization of the problem to treat advective–diffusive processes on variable spatial grids with nonlinear diffusion are treated in Brown and Pandolfo (1979, 1982), among others.

3. The numerical experiment

a. *The experimental data*

A comprehensive air/ocean/land data set was prepared for a full three-dimensional (limited-area) version of the model representing most of the GATE A-scale region. (Three-dimensional model experiments will be described in a forthcoming paper.) Because of the substantial effort involved in constructing time-varying boundary values for the full model, the simulation period was limited to the two days, 0000 GMT 4 September–0000 GMT 6 September 1974. It is this simulation period that is used for the one-dimensional-model experiments described in the following section.

For the one-dimensional case, data were evaluated at and about the position (7°4′N, 23°30′W) of the *Researcher* during GATE, Period III (see Fig. 1).

Input for the model includes: 1) initial vertical profiles of the wind/current components u and v, temperature T, specific humidity q (for the atmosphere) and salinity s (for the ocean); 2) lateral boundary values, which were linearly interpolated in time between 12-hourly values of horizontal gradients of u, v, T, q/s at each vertical grid level; and 3) horizontal pressure gradients at the upper boundaries of the air and water layers, estimated from linearly interpolated (in time) 12-hourly values of wind and current by employing the geostrophic approximation at these levels. Upper and lower boundary values of the dependent variables were also linearly interpolated in time between the 12-hourly values contained in the Global Data Sets. Initial values of the dependent variables and their horizontal derivatives are tabulated in the Appendix. Cloudiness and radiation are calculated from the model equations in accordance with existing conditions with respect to temperature, moisture, etc.

For the atmosphere, required data were derived by interpolation procedures from the GFDL GATE Version III 4-D Global Data Set. Horizontal gradients were computed by averaging finite-difference approximations to derivatives over five neighboring

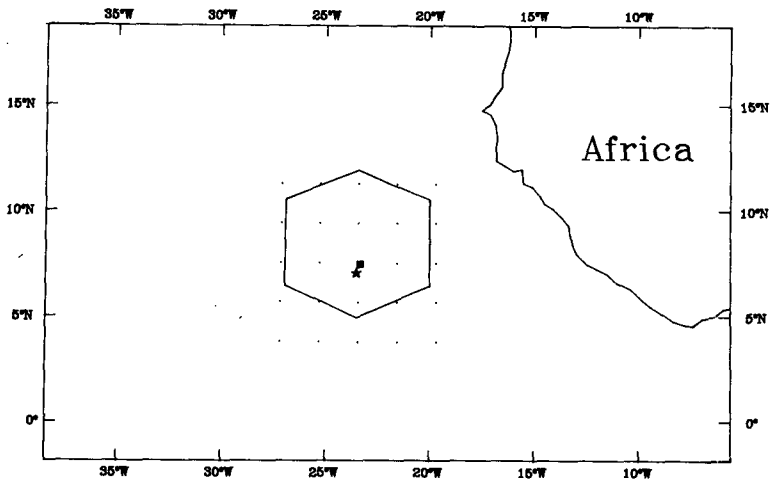

FIG. 1. Location of grid point (dark square) used in experiment. Position of grid point is shown relative to GATE AB-scale region (hexagon), the *Researcher* (star) and neighboring GFDL grid points (dots).

horizontal grid points centered on the Global Data Set grid point nearest the *Researcher* position. It should be noted that this evaluation defines the approximate atmospheric horizontal scale of the local numerical model (See Fig. 1). Atmospheric surface layer values of u and v and sea-surface values of T were obtained from the Bracknell Final Validated Data Set. Initial values of lower-level atmospheric variables (below 1000 mb) were computed by logarithmic interpolation in the vertical. For sub-surface depths down to −400 m, ship, mooring and atlas data were used to construct horizontal gradients of temperature, salinity and current components, while the STD measurements of the *Researcher* at initial time were used to construct initial profiles. Use of the Paulson-Simpson irradiance parameters (see Section 2b) requires the specification of a water type. For this experiment the clearest water type (Type IA) given by Jerlov (1968) as consistent with the location was specified.

The vertical grid used in the model is shown in Table 1. Also indicated are the grid levels of the GFDL GATE Version III data set from which initial values and time-dependent forcing functions were interpolated.

b. *Experimental results*

Among the general circulation models and the numerical prediction models which are the subject of the GATE Central Programme's second objective, and which are listed, e.g., in Pandolfo and Rowntree (1977), the model described above is unique in its method of coupling the air–sea boundary layers in such a way as to include the air–sea interface temperature as a solution variable. Therefore, this experiment was designed first to illustrate the degree of verisimilitude achievable in its numerical simulations of GATE sea-surface temperature, and subsequently, to illustrate its degree of sensitivity to the omission of the parameterized convective adjustments.

To this end, the experiment consisted of four model runs, each of which used a variant of the model summarily described in Section 2 above. The model variants used are labeled in Table 2.

The model-generated interface temperatures for each of these model variants are compared with two sets of measured sea-surface temperatures recorded at the *Researcher* during the 2-day simulation period, and corrected for systematic biases by Seguin *et al.* (1978). The difference between measured temperatures, consisting of a "bucket" set (giving the temperature of a bucket sample) and a "boom" set (giving the temperature sensed by a floating thermistor) provides an estimate of the observational uncertainty, approximately equivalent to that implied by the bias corrections of Seguin *et al.* (1978). In the remainder of this discussion, we shall refer to the model-generated interface temperature as "unrealistic" when it differs from *both* measured temperatures by more than the difference prevalent between measured temperatures, and as "realistic" when it differs from at least one of the measured temperatures by less than the prevalent difference between measured temperatures. It should be noted that Variant 1 is the model form previously shown to yield realistic calculations of interface temperature under steady, moderate wind conditions in an undisturbed Trade Regime (see, e.g., Jacobs and Brown, 1973). This model variant allows no parameterized "cloud and rain-out", and, consequently, no drying of the atmospheric layer, no cooling of the oceanic surface layers and no irregular modulation of the radiative

TABLE 1. (a) Vertical grid used in numerical experiments, and (b) relevant portion of vertical grid of GFDL GATE Version III data set.

(a)	(b)	
Z (m)	p (mb)	Z (m)*
	100.	16 694.
16 500.		
	150.	14 194.
	200.	12 389.
	250.	10 918.
10 500.		
	300.	9663.
	400.	7570.
7500.		
	500.	5865.
4500.		
	700.	3171.
3000.		
	800.	2053.
	850.	1538.
1500.		
	900.	1048.
1000.		
750.		
	950.	582.
500.		
250.		
	1000.	126.
125.		
75.		
25.		
10.		
1.		
0.		
−0.		
−1.		
−10.		
−20.		
−30.		
−40.		
−50.		
−75.		
−100.		
−150.		
−200.		
−300.		
−400.		

* 0000 GMT 4 September 1974, 7.5°N, 23°W.

fluxes. Thus, the finding of an erroneously warm model-generated temperature undergoing regular diurnal oscillation superimposed on a trend resulting from net local and advective warming, is not qualitatively surprising (see Fig. 2). To be noted are the properties that the differences between model-generated and measured temperatures generally exceed the differences between the two measured temperatures, that these differences generally increase with time, and that the "forecast error" has grown in two days to about a third of the accuracy requirement estimated in Charney *et al.* (1966).

The interface temperature generated by Model Variant 2 has the same general characteristics, as is shown in Fig. 3. Detailed comparison of Figs. 2 and 3 shows that the presence of a radiatively generated oceanic convective layer is manifested in detectably higher nighttime interface temperatures on the two nights subsequent to its first occurrence in the model.

In other words, use of the DP formulation allows diagnosis of a shallow insolation-induced thermocline in Model Variants 2 and 4 (see Fig. 7), which the basic finite-difference mesh (Table 1) is too coarse to resolve. The presence of this thermocline implies the persistence of a nocturnal inversion and accompanying convection within the uppermost grid layer until late into the second and third night (see Figs. 3 and 5). Its absence at initial time (0000 GMT), and the fact that our adaptation of the DP formulation could not bring it into play during the first 7 h of simulated nighttime, explains why Model Variants 2 and 4 are relatively more realistic during the second and third nights of simulation than they are during the first night. Deeper nocturnal inversion and convection conditions, resolvable by the basic grid, appear later in the night in Model Variants 2 and 4 and earlier in the day in Model Variants 1 and 3. This feature appears to yield more unrealistic nighttime interface temperatures for the odd-numbered variants (Figs. 4 and 5).

Fig. 4 shows that introduction of an atmospheric convective adjustment in Model Variant 3 results in much more obvious changes in model-generated interface temperature. Although there is still an unrealistically pronounced diurnal variation, it is not as regularly outlined, presumably due to the sporadic modulation of the modeled heat fluxes by the parameterized "cloud and rain-out." The daytime (hours 8–20, and 32–41) model-generated interface temperatures differ from at least one of the measured temperatures by less than the difference between measurement sets.

For Model Variant 4 (Fig. 5), this property is much more obvious. Except for the initial 3 h of the experiment and a few isolated hours thereafter, the model-generated interface temperature can be generally characterized as realistic, but showing more agreement with the boom temperature measurements than with the bucket measurements.

TABLE 2. Model variants used in the experiment.

Number	Description
1	Contains neither atmospheric nor oceanic convective adjustment
2	Contains no atmospheric convective adjustment
3	Contains no oceanic convective adjustment
4	Contains both atmospheric and oceanic convective adjustments

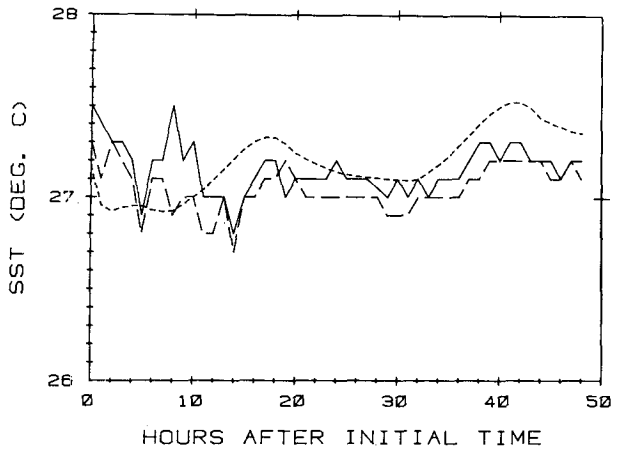

FIG. 2. Observed and computed sea-surface temperatures vs. time (initial time 0000 Z, 4 September 1974). Shown are bucket temperature (solid line), boom temperature (long-dashed line) and model-generated temperature (short-dashed line) computed with Variant 1 (no convective adjustment).

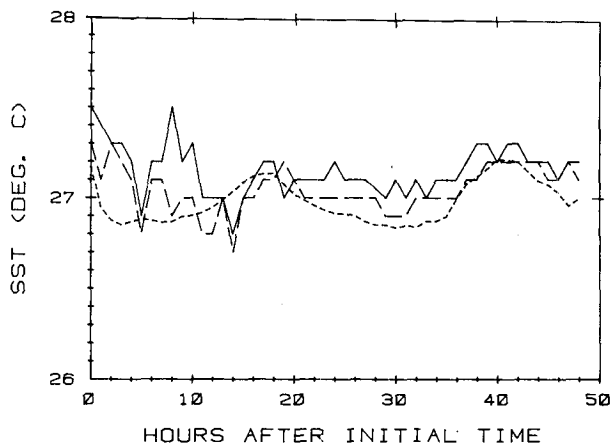

FIG. 4. As in Fig. 2 but with model Variant 3 (atmospheric convective adjustment).

The summary graph (Fig. 6) allows direct comparison of the model variant interface temperatures, as well as general comparison of model generated interface temperatures with the measured sea-surface temperatures. A key feature to be noted is that inclusion of the atmospheric convective adjustment (in Model Variants 3 and 4) enhances the sensitivity of modeled interface temperature to the presence of the oceanic convective adjustment. This is one example of the type of interactive effect of combined parameterizations on numerical model solutions that is frequently encountered, and that may in this case very well correspond to a natural interaction whose effects are not immediately perceptible to physical intuition.

The sensitivity of the modeled oceanic convective depth to the inclusion of the atmospheric convective adjustment is evident in Fig. 7. The presence of parameterized "cloud and rain," appears to deepen what might be called the "meteorologically active" layer of the modeled upper ocean by a significant amount, in terms of atmospheric thermal energy. The oceanic convective depth of Model Variant 2 exhibits approximately the diurnal "top-hat" variation predicted by Woods (1980) for clear conditions. This is significantly complicated by the inclusion of the atmospheric convective adjustment in Model Variant 4.

The sensitivity of the modeled atmospheric condensation level to the inclusion of the oceanic adjustment is shown in Fig. 8, and in greater detail at low levels in Fig. 9. This sensitivity is not as pronounced as that shown in Fig. 7, except at the very end of the integration period. It should be noted, however, that the oceanic convective adjustment did not become active until the 9th hour of integration (see Fig. 5).

The physical bases of the differences among model solutions of the four variants lie in the complex set

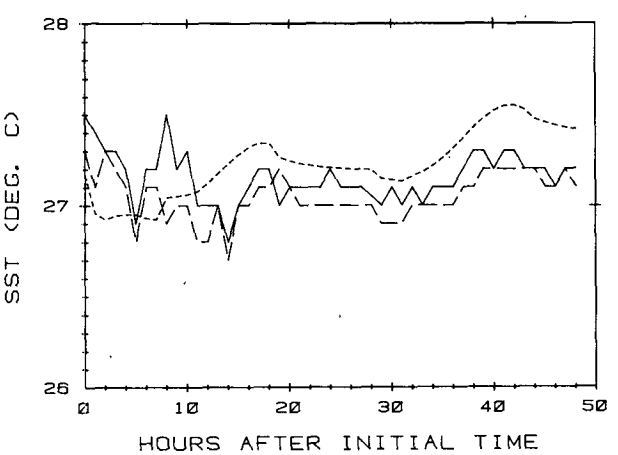

FIG. 3. As in Fig. 2 but with model Variant 2 (oceanic convective adjustment).

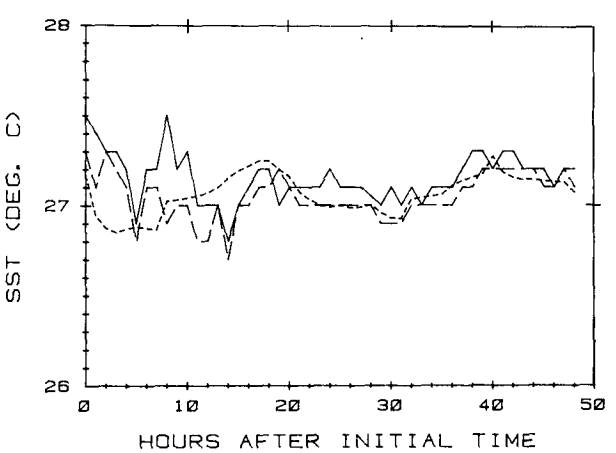

FIG. 5. As in Fig. 2 but with model Variant 4 (atmospheric and oceanic convective adjustment).

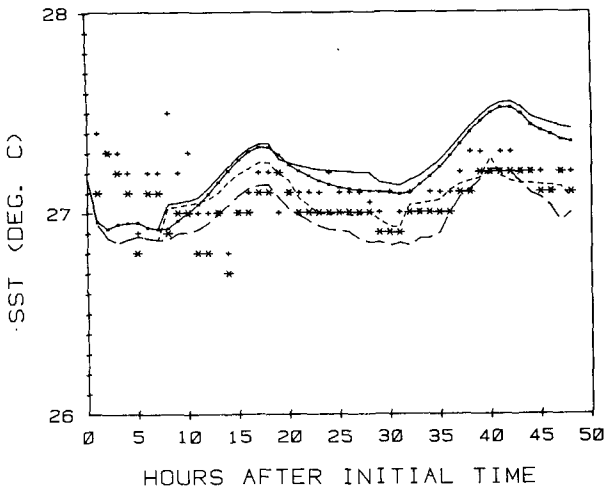

FIG. 6. Model-generated sea-surface temperatures as a function of time for model Variants 1 (dotted line), 2 (solid line), 3 (long-dashed line) and 4 (short-dashed line). Bucket (crosses) and boom (asterisks) temperatures are shown as discrete data points.

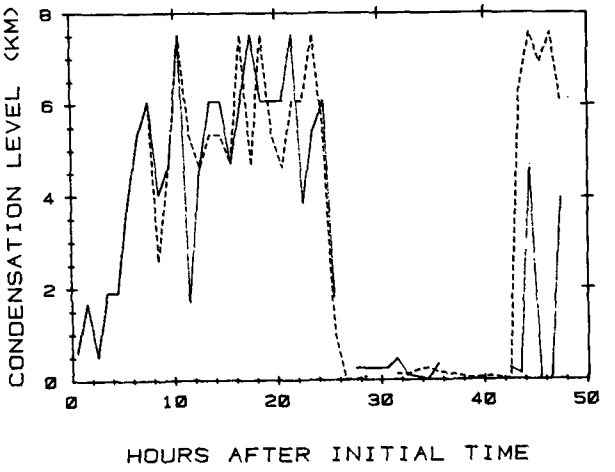

FIG. 8. Model-generated atmospheric condensation level computed with model Variants 3 (solid line) and 4 (dashed line). Variant 4 contains oceanic convective adjustment while Variant 3 does not.

of direct and indirect interactions introduced by the convective adjustment processes acting alone, or acting jointly. In the case studied, three potential scaling lengths are used in the numerical model of oceanic mixing: the Monin-Obukhov "stability" length; the Kitaigorodsky "turbulent wave" length; and the Dalu-Purini "insolation–convection depth." The interplay among the three yields more realistically irregular time-series of model-generated interface temperature than does the interaction of just the first two (compare Figs. 2 and 3, or 4 and 5). Qualitatively, presence of the shallow insolation-induced thermocline, when allowed by weak wind-mixing conditions, can be seen to produce extended periods of gradual temperature change, until its appearance or disappearance produced abrupt transitions.

Inspection of the interface heat balance equation used in the model (Jacobs and Brown, 1973) identifies several possible counteracting direct effects of atmospheric cloud and rain on the interface temperature. A tendency toward cooling is produced by the reduction of insolation by cloud, while a tendency toward warming is produced by the augmentation of downward atmospheric radiative flux by cloud. Rain impinging on the surface may produce either warming or cooling depending on the sign of the difference between low-level atmospheric wet bulb temperature and the interface temperature. These are just the most obvious direct effects. Since the formation of cloud and rain in the atmospheric layer requires latent heat release, consequent atmospheric warming, and the removal of water vapor, there can be many important indirect effects, e.g., enhanced evaporation from the interface and suppressed sensible heat flux from the ocean to the atmosphere. In

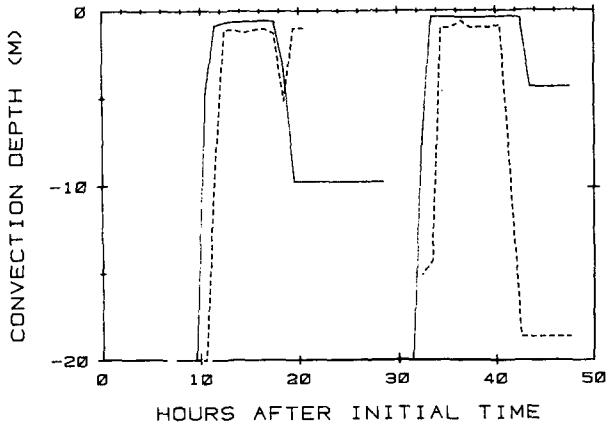

FIG. 7. Model-generated oceanic convective depth computed with model Variants 2 (solid line) and 4 (dashed line). Variant 4 includes atmospheric convective adjustment while Variant 2 does not.

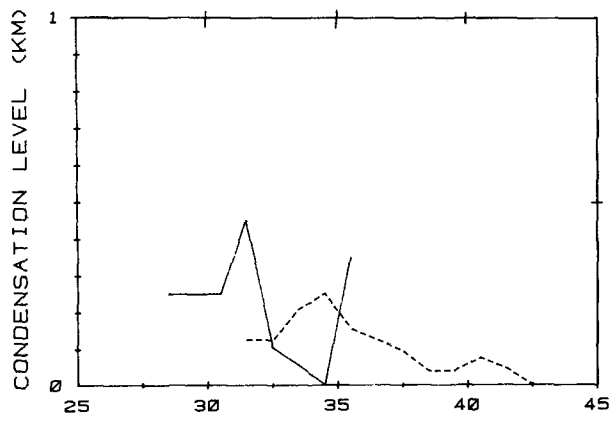

FIG. 9. As in Fig. 8 but with results shown in greater detail for 27.5–42.5 h after initial time.

any given case, at any given time, a few of these effects may be dominant, but there is no way to judge the net effect in general by relying on physical intuition. In the case studied, the prevalent net effects are to produce relative cooling and more irregular variation of the interface temperature solution (compare Figs. 2 and 4, or 3 and 5). The dominant processes accounting for these features of the model solutions are the reduction of insolation by cloud, and the enhancement of evaporation by convection-induced atmospheric drying. There is no reason to suppose that this picture does not, at least qualitatively, correspond to what actually happened in nature in the case considered.

4. Conclusion

The experimental model used, as outlined in Sections 2a–3b is the result of a linked sequence of selections of individual model elements, beginning with the choice of a model core consisting of the primitive equations in Eulerian form, and ending with the selection of one water type for the experiment out of seven listed in Table 2 of Paulson and Simpson (1977). It should, therefore, be pointed out that this is a common property of the present array of operating numerical models used in general circulation studies and in numerical weather prediction, and that it cannot be avoided in any direct attempt to further the second objective of the GATE Central Programme. It is also pointed out that while the particular selections made differ in detail from those used in any of the other individual numerical models described in the references cited, they do not differ to any qualitatively greater degree than these other models differ from each other.

The generally realistic interface temperatures achieved do *not* justify a conclusion that any single model element used here (e.g., the oceanic convective parameterization) is, in its detailed form, preferable for use in any other model, or, indeed, that it is the optimum form for the model used here. We presume, however, that the potential improvement that might be provided by refinements of the detailed form lies within the range of sensitivity defined by the solutions of the model variants already considered.

The results do suggest that coupling of the uppermost oceanic and atmospheric boundary layer in models containing stability dependent formulations for the small-scale vertical turbulent flux; parameterized cloud and radiation interactions; parameterized treatment of atmospheric latent heating and drying, and enhanced oceanic vertical heat transports due to sub-model scale convective phenomena; and greater vertical resolution than is common in the present array of operating global scale models could allow the multi-day numerical prediction of sea-surface temperature with accuracy comparable to the uncertainty of measurement in tropical marine regimes similar to that prevalent during GATE Period III.

The simple technique used in the experiment described here was one-dimensional nesting, of a locally detailed model at a selected single horizontal mesh point of a global-scale data base, with the local model being supplied with time-varying horizontal gradients of the dependent variables by the large-scale data set. While the technique was sufficient for this preliminary experiment, the practical and internally consistent implementation of all the listed refinements in a global-scale, primitive-equation model would represent a significant effort in numerical modeling technology. As a next step we have constructed a three-(space) dimensional version of the local model to be nested in the GATE global-scale data set. Extension of the nested model's spatial domain will allow a direct computational link between horizontal fields of convectively adjusted temperature and humidity, and the horizontal advection of these variables, which is lacking in the local model. Further experiments with this coupled air–sea interaction limited-area model will be described in forthcoming papers.

Acknowledgments. This material is based upon work supported by the Division of Atmospheric Sciences, National Science Foundation under Grant ATM-7824273. Atmospheric data sets were provided by the Geophysical Fluid Dynamics Laboratory of the NOAA and the United Kingdom Meteorological Office to whom we are most grateful. Oceanic data sets were prepared by Dr. Clifford A. Jacobs under National Science Foundation Grant ATM-7825303. Solar and infrared radiation routines were designed by Dr. Marshall A. Atwater and Mr. John T. Ball under National Science Foundation Grant ATM-7707504. Model experiments were performed using the computer facility of the National Center for Atmospheric Research, which is sponsored by the National Science Foundation. The authors wish to thank Dr. Alfonso Sutera and Dr. G. A. Dalu for helpful discussions. Thanks are also extended to Mr. David Adamec for assisting in the computer graphics and to Ms. Margaret Atticks for typing the manuscript.

APPENDIX

Initial Profiles of Dependent Variables and Derivatives

In the tables containing the horizontal derivatives, data for the interior ocean layers are not shown. The required values are constructed by linear interpolation between the data points at the ocean surface (0 m) and the lowest depth (−400 m).

TABLE. Atmospheric and oceanic data sets.

Height/Depth (m)	u (cm s^{-1})	v (cm s^{-1})	T (°C)	$q(s)$ (g kg^{-1})
16500.	−330.07	211.77	−72.51	0.01
10500.	−823.80	−706.74	−39.81	0.01
7500.	−300.99	−92.69	−16.56	0.74
4500.	−560.44	262.82	0.08	4.69
3000.	−640.11	398.60	8.28	7.19
1500.	−88.67	234.32	16.45	11.98
1000.	199.84	246.23	19.17	13.91
750.	273.56	212.32	20.33	14.86
500.	336.27	217.12	21.68	15.76
250.	376.01	300.48	23.43	16.56
125.	395.19	341.24	24.30	16.95
75.	376.53	323.39	24.45	17.23
25.	336.32	284.73	24.79	17.82
10.	302.78	252.49	25.07	18.31
1.	218.51	171.48	25.77	19.55
0.	217.01	170.03	27.17	22.03
0.	217.01	170.03	27.17	35.30
−1.	49.96	9.45	27.17	35.30
−10.	49.96	9.45	27.19	35.38
−20.	41.39	8.88	27.20	35.51
−30.	36.86	14.73	27.03	35.64
−40.	25.61	6.19	25.99	35.84
−50.	25.15	12.52	24.61	35.92
−75.	34.08	−0.16	17.87	35.72
−100.	20.15	6.66	15.49	35.55
−150.	21.16	3.83	13.85	35.42
−200.	20.75	4.76	12.73	35.29
−300.	15.13	2.04	11.36	35.12
−400.	16.07	6.44	10.23	35.05
	u_x (s^{-1})	u_y (s^{-1})	v_x (s^{-1})	v_y (s^{-1})
16500.	0.0	0.0	0.0	0.0
10500.	−0.2107 (−5)	−0.3955 (−5)	−0.2396 (−5)	0.1982 (−5)
7500.	0.3287 (−5)	−0.2141 (−5)	0.2839 (−5)	0.3711 (−5)
4500.	−0.3481 (−5)	−0.3743 (−5)	−0.3429 (−5)	0.4012 (−5)
3000.	−0.4911 (−5)	−0.1570 (−5)	−0.6394 (−5)	0.3674 (−5)
1500.	0.4213 (−6)	0.5443 (−6)	−0.1333 (−5)	−0.1571 (−5)
1000.	−0.1138 (−5)	0.1538 (−5)	0.1023 (−5)	−0.1484 (−5)
750.	0.1370 (−5)	0.1924 (−6)	0.1905 (−5)	−0.1682 (−5)
500.	0.2783 (−5)	−0.4136 (−6)	0.2576 (−5)	−0.2044 (−5)
250.	0.1589 (−5)	0.6519 (−6)	0.2743 (−5)	−0.2889 (−5)
125.	0.9874 (−6)	0.1178 (−5)	0.2825 (−5)	−0.3311 (−5)
75.	0.9225 (−6)	0.1109 (−5)	0.2698 (−5)	−0.3167 (−5)
25.	0.8524 (−6)	0.9480 (−6)	0.2349 (−5)	−0.2796 (−5)
10.	0.7941 (−6)	0.8135 (−6)	0.2058 (−5)	−0.2487 (−5)
1.	0.6473 (−6)	0.4755 (−6)	0.1327 (−5)	−0.1710 (−5)
0.	0.3536 (−6)	−0.2005 (−6)	−0.1349 (−6)	−0.1558 (−6)
0.	0.3536 (−6)	−0.2005 (−6)	−0.1349 (−6)	−0.1558 (−6)
−400.	0.0	0.0	0.0	0.0
	T_x (°C cm^{-1})	T_y (°C cm^{-1})	$q_x(s_x)$ (g kg^{-1} cm^{-1})	$q_y(s_y)$ (g kg^{-1} cm^{-1})
16500.	0.6343 (−7)	−0.3655 (−7)	0.0	0.0
10500.	−0.4407 (−7)	0.2615 (−7)	−0.2511 (−10)	0.1669 (−8)
7500.	0.1819 (−7)	−0.4109 (−8)	0.2359 (−8)	0.6289 (−8)
4500.	−0.3317 (−7)	−0.6827 (−8)	0.5060 (−8)	0.1607 (−7)
3000.	0.2172 (−7)	0.1105 (−9)	0.8414 (−8)	0.2547 (−7)
1500.	−0.7875 (−8)	0.4638 (−7)	0.2547 (−7)	0.3551 (−7)
1000.	0.4863 (−8)	0.2659 (−7)	0.2285 (−7)	0.1789 (−7)
750.	0.1229 (−7)	0.1070 (−7)	0.2285 (−7)	0.1398 (−7)
500.	0.1320 (−7)	0.7166 (−8)	0.2134 (−7)	0.1110 (−7)
250.	0.6868 (−8)	0.5519 (−8)	0.1624 (−7)	0.1073 (−7)
125.	0.3665 (−8)	0.4631 (−8)	0.1370 (−7)	0.1057 (−7)
75.	0.3382 (−8)	0.4725 (−8)	0.1270 (−7)	0.1070 (−7)
25.	0.2578 (−8)	0.5278 (−8)	0.1067 (−7)	0.1084 (−7)
10.	0.1907 (−8)	0.5739 (−8)	0.8980 (−8)	0.1095 (−7)
1.	0.2213 (−9)	0.6899 (−8)	0.4731 (−8)	0.1124 (−7)
0.	−0.3150 (−8)	0.9218 (−8)	−0.3767 (−8)	0.1181 (−7)
0.	−0.3150 (−8)	0.9218 (−8)	−0.3767 (−8)	0.1181 (−7)
−400.	0.0	0.0	0.0	0.0

REFERENCES

Arakawa, A., and W. H. Schubert, 1974: Interaction of a cumulus cloud ensemble with the large-scale environment, Part 1. *J. Atmos. Sci.*, **31,** 674–701.

Atwater, M. A., 1972: Thermal effects of urbanization and industrialization in the boundary layer. A numerical study. *Bound.-Layer Meteor.*, **3,** 229–249.

——, and P. S. Brown, Jr., 1974: Numerical computations of the latitudinal variation of solar radiation for an atmosphere of varying opacity. *J. Appl. Meteor.*, **13,** 289–297.

Ball, J. T., M. A. Atwater and S. J. Thoren, 1981: Sensitivity of computed incoming solar radiation at the surface to cloud analyses. *Mon. Wea. Rev.*, **109,** 203–208.

Brown, P. S., Jr., and J. P. Pandolfo, 1978: Merging finite-difference schemes having dissimilar time-differencing operators. *Mon. Wea. Rev.*, **106,** 268–270.

——, and ——, 1979: Numerical stability of the combined advection–diffusion equation with nonuniform spatial grid. *Mon. Wea. Rev.*, **107,** 959–962.

——, and ——, 1980: A gravity wave problem with the upstream difference method. *J. Comput. Phys.*, **37,** 141–150.

——, and ——, 1982: A numerical predictability problem in solution of the nonlinear diffusion equation. Submitted to *Mon. Wea. Rev.*

Charney, J., *et al.*, 1966: The feasibility of a global observation and analysis experiment. Rep. of the Panel on International Meteorological Cooperation. COS, Intern. Acad. Sci., National Research Council, Washington, DC, Nat. Acad. Sci. Publ. 1290, 172 pp.

Dalu, G. A., and R. Purini, 1982: Convection depth and surface temperature anomalies in the ocean. *Quart. J. Roy. Meteor. Soc.* (in press).

Gray, W. M., and R. W. Jacobson, 1977: Diurnal variation of deep cumulus convection. *Mon. Wea. Rev.*, **105,** 1171–1188.

Greenfield, R. S., and J. S. Fein, 1979: The Global Atmospheric Research Program's Atlantic Tropical Experiment. *Rev. Geophys. Space Phys.*, **17,** 1762–1771.

Houghton, D. D., 1974: The Central Programme for the GARP Atlantic Tropical Experiment. Global Atmospheric Research Program, GATE Rep. No. 3, 35 pp.

Jacobs, C. A., 1978: Numerical simulations of the natural variability in water temperature during BOMEX using alternative forms of the vertical eddy exchange coefficients. *J. Phys. Oceanogr.*, **8,** 119–141.

——, and P. S. Brown, Jr., 1973: An investigation of the numerical properties of the surface heat balance equation. *J. Appl. Meteor.*, **12,** 1069–1072.

Jerlov, N. G., 1968: *Marine Optics.* Elsevier/North-Holland, 231 pp.

Kasahara, A., 1961: A numerical experiment on the development of a tropical cyclone. *J. Meteor.*, **18,** 259–282.

Kraus, E. B., and J. S. Turner, 1967: A one-dimensional model of the seasonal thermocline II. *Tellus*, **19,** 98–105.

Kreitzberg, C. W., and D. J. Perkey, 1976: Release of potential instability; Part I: A sequential plume model within a hydrostatic primitive equation model. *J. Atmos. Sci.*, **33,** 456–475.

Krishnamurti, T. N., H. L. Pan, C. B. Chang, J. Ploshay, D. Walker and A. W. Oodally, 1979: Numerical weather prediction for GATE. *Quart. J. Roy. Meteor. Soc.*, **105,** 979–1010.

Lilly, D. K., 1962: On the numerical simulation of buoyant convection. *Tellus*, **14,** 148–172.

Lyne, W. H., P. R. Rowntree, C. Temperton and J. Walker, 1976: Numerical modeling using GATE data. *Meteor. Mag.*, **105,** 261–271.

Manabe, S., J. Smagorinsky and R. F. Strickler, 1965: Simulated climatology of a general circulation model with a hydrological cycle. *Mon. Wea. Rev.*, **93,** 769–798.

McDonald, J. E., 1963: The saturation adjustment in numerical modeling of fog. *J. Atmos. Sci.*, **20,** 470–478.

McGarry, M. M., and R. J. Reed, 1978: Diurnal variations in convective activity and precipitation during Phases II and III of GATE. *Mon. Wea. Rev.*, **106,** 101–113.

Miyakoda, K., and J. Sirutis, 1977: Comparative integrations of global models with various parameterized processes of subgrid-scale vertical transports: description of parameterizations. *Beitr. Phys. Atmos.*, **50,** 445–447.

——, —— and J. Sheldon, 1980: The four-dimensional analysis and forecast experiment with GATE data. *Proc. Seminar on the Impact of GATE on Large-Scale Numerical Modeling of the Atmosphere and Ocean.* U.S. Committee for GARP, Woods Hole, 265–272.

Niiler, P. P., and E. B. Kraus, 1977: One-dimensional models of the upper ocean. *Modelling and Prediction of the Upper Layers of the Ocean*, E. B. Kraus, Ed., Pergamon Press, 325 pp.

Pandolfo, J. P., 1969: Motions with inertial and diurnal period in a numerical model of the navifacial boundary layer. *J. Mar. Res.*, **27,** 301–317.

——, 1971: Numerical experiments with alternative boundary layer formulations using BOMEX data. *Bound.-Layer Meteor.*, **1,** 277–289.

——, and C. A. Jacobs, 1972: Numerical simulations of the tropical air–sea planetary boundary layer. *Bound.-Layer Meteor.*, **3,** 15–46.

——, and P. Rowntree, 1977: Large-scale numerical modeling. Rep. U.S. GATE Central Program Workshop, Boulder, 90–122.

Paulson, C. A., and J. J. Simpson, 1977: Irradiance measurements in the upper ocean. *J. Phys. Oceanogr.*, **7,** 952–956.

Peters, H., 1978: On the variability of the near-surface oceanic layer in the Intertropical Convergence Zone. *Oceanol. Acta*, **1,** 305–314.

Ramanathan, V., and R. E. Dickinson, 1981: A scheme for forming nonprecipitating low-level clouds in GCM's. Rep. of the Workshop on Clouds in Climate: Modeling and satellite observational studies, NASA/Goddard Inst. Space Studies, New York, 85–87.

Richtmyer, R. D., and K. W. Morton, 1967: *Difference Methods for Initial-Value Problems.* Interscience, 405 pp.

Seguin, W. R., R. B. Crayton, P. Sabol and J. W. Carlile, 1978: *GATE Convection Subprogram Data Center.* Final Rep. on Ship Surface Data Validation, NOAA Tech. Rep. EDS25, 77 pp.

Shukla, J., and Y. Sud, 1981: Effect of cloud–radiation feedback on the climate of a general circulation model. Rep. of the Workshop on Clouds in Climate: Modeling and satellite observational studies, NASA/Goddard Inst. Space Studies, New York, 42–48.

Wetherald, R. T., and S. Manabe, 1981: Simulations of cloud cover with a general circulation model of the atmosphere. Rep. of the Workshop on Clouds in Climate: Modeling and satellite observational studies, NASA/Goddard Inst. Space Studies, New York, 27–33.

Woods, J. D., 1980: Diurnal and seasonal variation of convection in the wind mixed layer of the ocean. *Quart. J. Roy. Meteor. Soc.*, **106,** 379–394.